Universal properties of cuprate superconductors: T_c phase diagram, room-temperature thermopower, neutron spin resonance, and STM incommensurability explained in terms of Chiral Plaquette Pairing

Jamil Tahir-Kheli and William A. Goddard III

Materials and Process Simulation Center (MC 139-74)
California Institute of Technology, Pasadena CA 91125

jamil@wag.caltech.edu, wag@wag.caltech.edu

Supporting Information

Doping restrictions and its effect on the optimal doping value

Figure S1(a) shows the restricted plaquette doping used in this paper and figure S1(b) shows the more general doping.

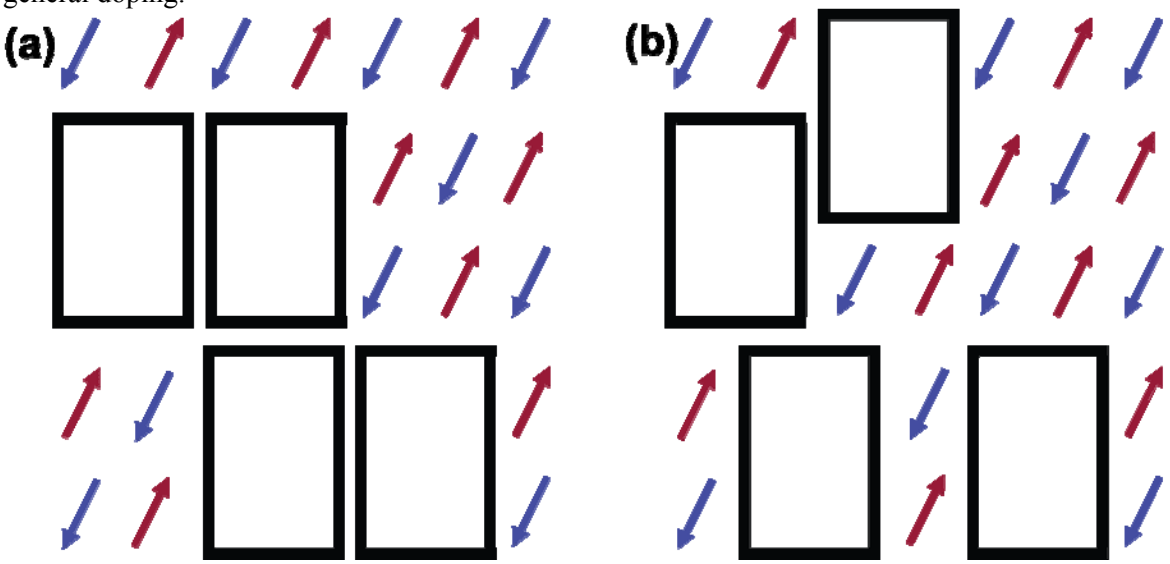

Figure S1. (a) restricted plaquette doping where the plaquettes centers are separated by an even number of lattice spacings. (b) general plaquette doping with no overlap. This constraint can be fulfilled up to 0.187 doping.

The restricted doping in figure S1(a) can be doped all the way to x=0.25 where there are no remaining d^9 sites. For random doping of plaquettes in the general form of figure S1(b), we find that for x>0.187, it is not possible to satisfy the constraint of no overlap of the plaquettes. We calculate this value by randomly doping a large ensemble of 1000 X 1000 lattices and computing the doping where the constraint cannot be satisfied. This doping is significantly greater than our calculated optimal doping of 0.167.

The detailed location of the dopants in the cuprates is determined by details of the high-temperature fabrication and the annealing/quenching profile. For dopings less than 0.187, the Coulomb repulsion of the impurity dopants will lead to patches of restricted plaquettes as shown in figure S1(a) that are joined to patches shifted by one lattice spacing. Since the calculated optimal doping at 0.167 is well within the

regime where four-site plaquettes can be formed without overlap, our estimate of the optimal doping value is reliable.

It is interesting to continue doping beyond the plaquette overlap constraint for x<0.187. Assuming that the Coulomb repulsion of the dopant impurities will lead to further four-site plaquettes at locations that cover three d^9 spins, this constraint can be satisfied up to 0.226. Above x=0.226, the impurities lead to additional plaquettes that cover two d^9 spins. This constraint is exhausted at x=0.271. Finally, one-spin plaquettes can be doped up to x=0.317.

In the paper, we argued that at x=0.25 there are no longer any remaining d^9 spins to lead to superconducting pairing. In the more general doping picture described here, pairing will disappear when only isolated d^9 spins remain because the nearest-neighbor AF correlation (J_{dd}) that leads to pairing is lost. This occurs at x=0.271. Experiment is ≈0.27.

For the neutron resonance, thermopower, and STM incommensurability, the surface area of the plaquettes is unnecessary. Only average values for the spacing between plaquettes and d^9 regions are used. Thus the main results of the paper are not dependent on the details of the plaquette doping.

Integrated neutron spin susceptibility

The imaginary part of the magnetic susceptibility due to AF clusters of size n is given by $\chi''(q,\omega)$ where[1]

$$\frac{\chi_n''(q,\omega)}{(g\mu_B)^2} = \frac{\pi}{2}\cdot\frac{N_{clus}(n)}{N_{cells}} |<1|\, S^+(q)\,|0>|^2\ \delta(\hbar\omega - E_n).$$

$N_{clus}(n)$ is the number of clusters of size n, N_{cells} is the total cells, E_n is the cluster energy gap, g=2 is the g-factor, and $S^+(q) = \sum e^{iqR} S^+(R)$ is the Fourier transformed spin raising operator summed over the sites R in the finite cluster. The matrix element is between the ground state (S=0) and the lowest excited state (S=1). The units are μ_B^2/eV/f.u. Integrating over energy removes the delta function in the above expression. The energy integrated susceptibility is the sum over all clusters

$$\int d\omega \chi''(q,\omega) = \sum_n \int d\omega \chi_n''(q,\omega).$$

To determine the matrix element in the equation, we computed the S=0 ground state and S=1 first excited state for all AF cluster shapes and sizes up to 24 spins. The four-site plaquette doping as shown in figure S1(a) leads to finite clusters comprised of 4, 8, 12, 16, … d^9 sites. The nearest-neighbor AF spin coupling is the same as for undoped systems, J_{dd} = 130 meV. There are no periodic boundary conditions applied to calculate the ground state to first excited state energy splitting.

We computed the energy splitting for all possible AF clusters up to 24 spin sites. The ground state is determined by diagonalizing the S=0 spin state that has 2,704,156 terms. Lanczos diagonalization is used. This leads to the ground state energy. Since the neutron resonance is a spin-flip scattering, the lowest energy state with S=1 is the excited state that is probed by the neutrons. A second Lanczos diagonalization to determine the ground state in the state space of S=1 with 2,496,144 states is performed. The difference is the energy splitting.

Figure S2 shows all the possible AF d^9 clusters possible up to 20 sites and figure S3 shows all the 24-site clusters. For each size, the probability of each cluster shape was determined in addition to the S=0 ground state to S=1 energy splitting. The probabilities and energies were used to determine the mean energy splitting for each cluster size.

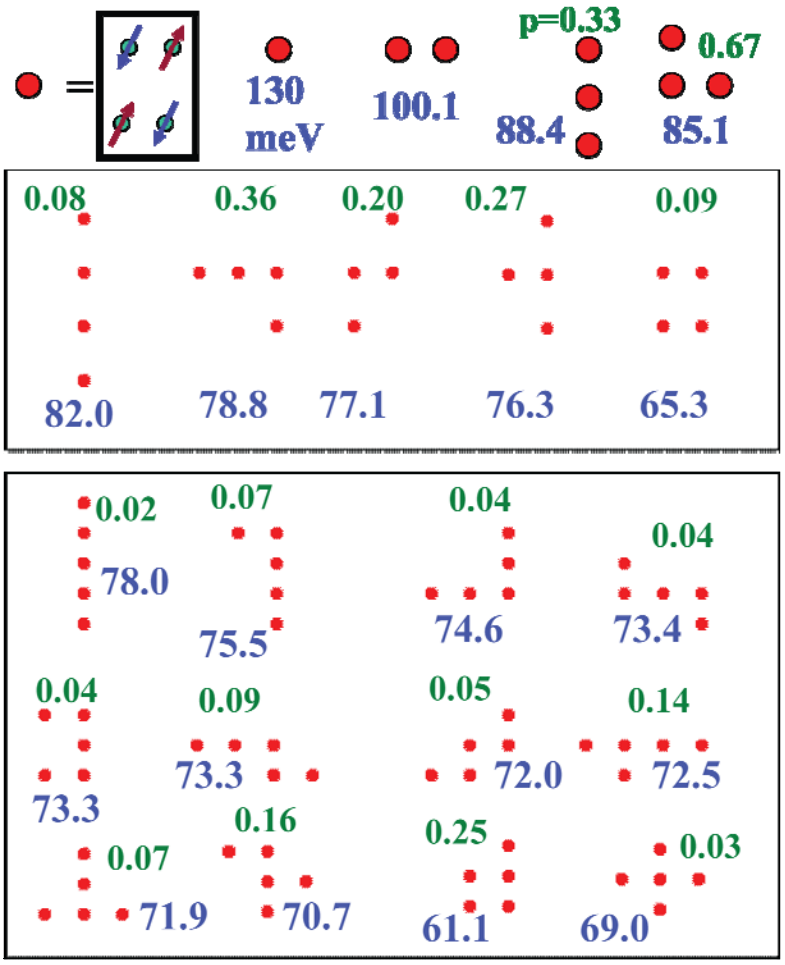

Figure S2. All 4, 8, 12, 16, and 20 AF d^9 site clusters. The red dot expands to four d^9 spins as shown in the upper left corner. The ground state to S=1 excited state energy is shown in meV in blue and the probability of the cluster is shown in green. The undoped spin-spin coupling, J_{dd} = 130 meV, is used in these calculations. There is only one 4-site and 8-site cluster. There are 2, 5, and 12 clusters for 12, 16, and 20 sites, respectively.

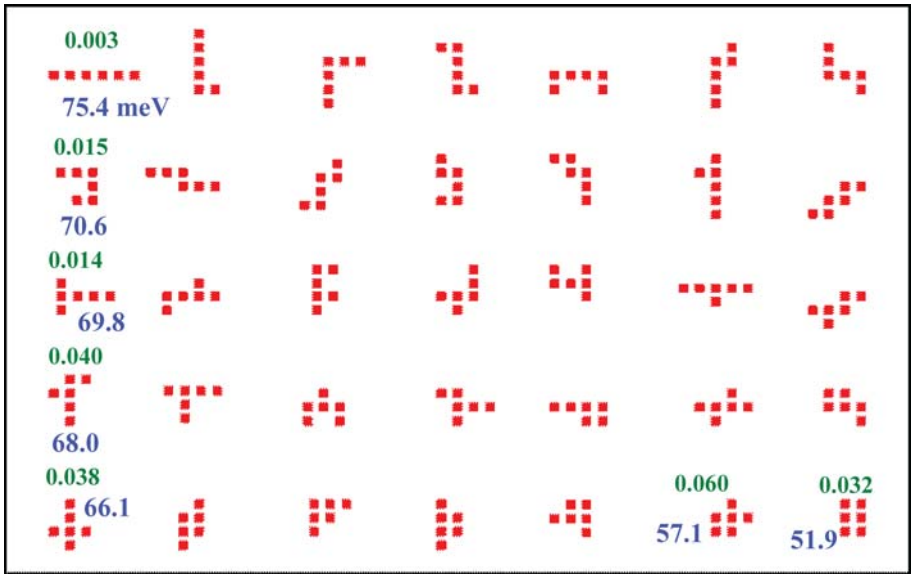

Figure S3. The 35 possible 24-site AF d^9 spin clusters. The energy splitting is shown in blue and the probability is in green. The most probable cluster is the second to last cluster on the lower right with energy splitting of 57.1 meV and probability 0.06. The clusters are arranged from highest energy splitting to lowest.

24-site AF d^9 clusters are too small to include all the cluster sizes that can appear for the superconducting range of dopings. Thus we must extrapolate our energies to larger clusters.

Since the spin-wave dispersion is linear in momentum, $\omega \sim k$, and the smallest k in a finite cluster is $\sim N^{-1/2}$, where N is the cluster size, we expect our calculated energy splittings to be fitted by a power series in $N^{-1/2}$. The mean energy as a function of N and a fit to the data with the first two terms in the power series in $N^{-1/2}$ is shown in figure S4. The fit is excellent with an RMS error of 0.61 meV and a maximum percentage error of 1.03%.

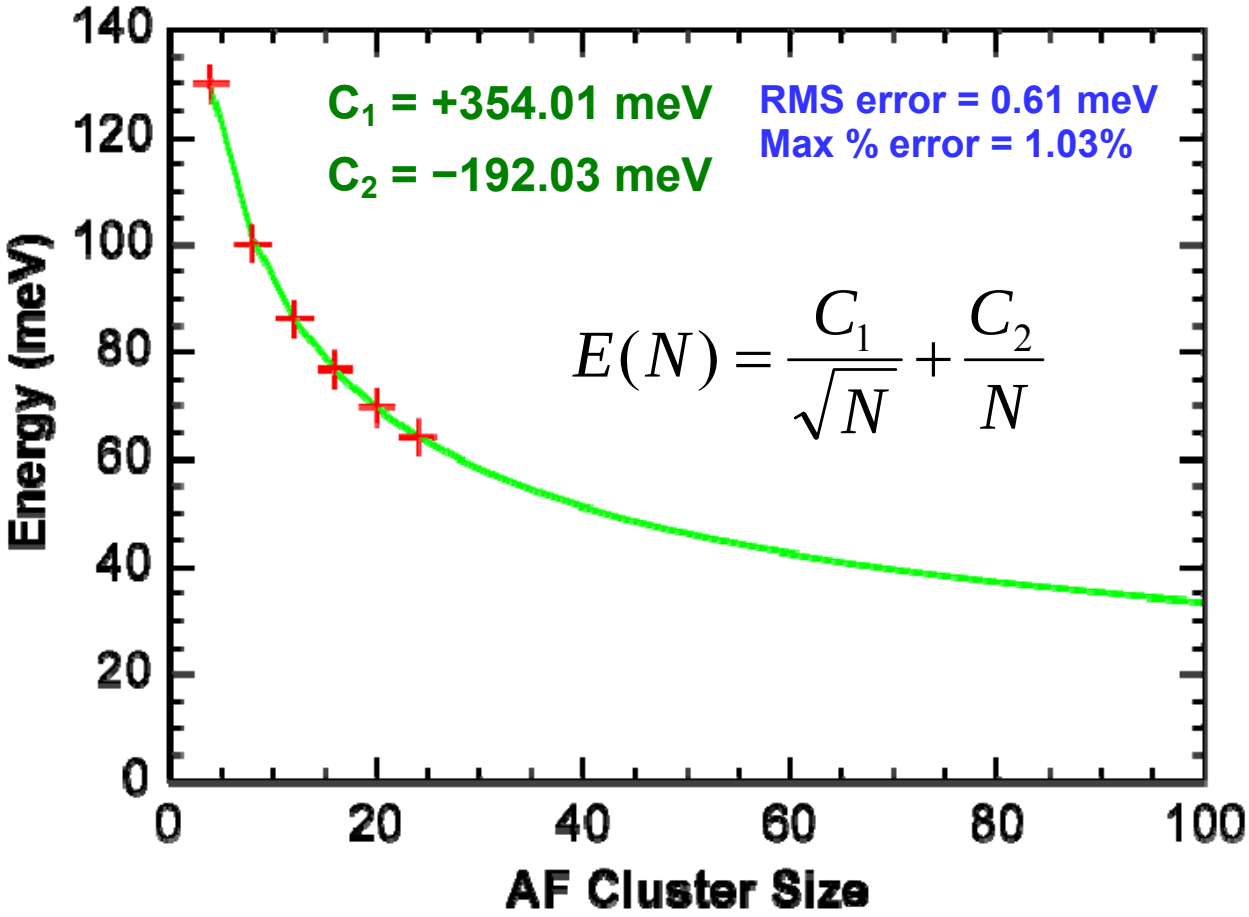

Figure S4. Fit of the mean energy for cluster sizes up to 24-sites with the first two terms in a power series expansion in $N^{-1/2}$ where N is the cluster size. An $N^{-1/2}$ series expansion is expected from spin-wave theory. The fit is excellent using only the first two terms in the series. The maximum error is 1.03 meV and the RMS error is 0.61 meV. The largest percentage error of the six data points is 1.03%. Note that the coefficient C_2 is negative.

From spin-wave theory, the matrix element, $\frac{1}{n}|<1|S^{+}(q)|0>|^2$, increases to infinity with increasing n. We used our eigenstates for clusters up to 24 AF spins to calculate this term for q=(π,π). This term fits the power law Cn^{α} with an RMS error of 0.01 and maximum percentage error of 0.59%, where C=0.86 and α=0.32 as shown in figure S5. An interesting observation is that the expression CN^{α} is very close to $(4/3)(N/4)^{1/3}$.

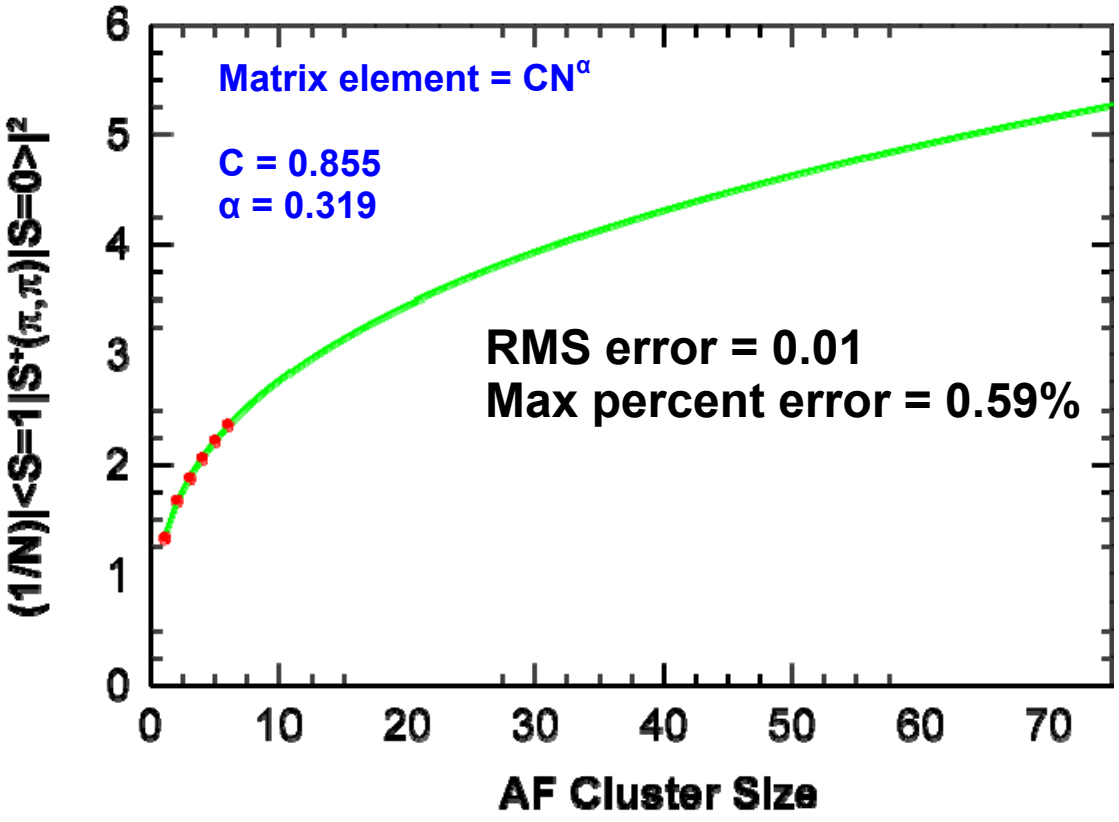

Figure S5. Calculated matrix element of the spin raising operator at momentum (π, π) for all possible clusters up to 24 undoped AF d^9 spins. The curve is very well fit by the power law expression, CN^{α}, where C = 0.855 and α = 0.319. The RMS error is 0.01 and the maximum percentage error is 0.59%.

Finally, to compute the integrated susceptibility, we need to know how many clusters there are of each size in the material. We calculated the number of clusters of size n, $N_{clus}(n)$, by randomly doping 1000 ensembles of a 2000 X 2000 lattice. The results are shown in figure S6. The values were determined by averaging over 1000 ensembles. The figure shows the results for dopings x = 0.16 and x = 0.10. Only the x = 0.16 data is used in the main text.

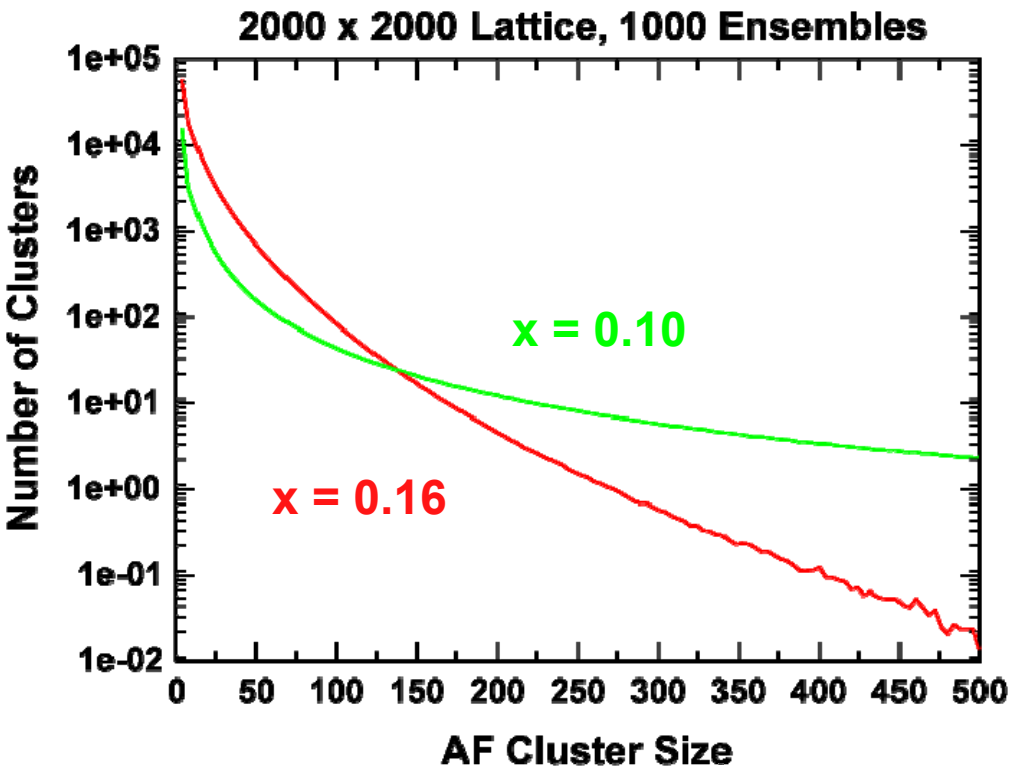

Figure S6. The number of clusters of each size for dopings of x = 0.16 and 0.10. For x = 0.16, there are fewer undoped d^9 sites leading to fewer large-sized clusters than x = 0.10. The curves in the figure were calculated for a 2000 x 2000 lattice and averaging was done over 1000 ensembles. The y-axis (number of clusters) is plotted on a log scale and is not normalized by the number of lattice sites. If the lattice size was doubled, the number of clusters would double.

Calculation of neutron resonance width

The S=1 state excited by the neutron decays by electron-spin scattering with the x^2-y^2/pσ band electrons. The width of the resonance peak, Γ (half-width at half-maximum, HWHM), is given by $\Gamma=\pi|W|^2F_{BCS}$ where F_{BCS} is the standard electron spin-flip scattering term with BCS coherence factors[2]. $|W|^2=|M|^2(1-\lambda)/2(1-\lambda)^{1/2}$ where $\lambda=[1-(E_{res}/2J_{dd})^2]^{1/2}$ and the matrix element $M\approx J_{dd}{}^3$. For the bilayer systems, F_{BCS} only includes scattering between the bonding and anti-bonding bands.

References

[1] P. Bourges et al, Phys. Rev. B. **56**, R11439 (1997)
[2] D. K. Morr and D. Pines, Phys. Rev. Lett. **81**, 1086 (1998).
[3] E. Manousakis, Rev. Mod. Phys. **63**, 1 (1991).